Polycyclic aromatic hydrocarbons (PAHs) in continental shelf sediment of China: Implications for anthropogenic influences on coastal marine environment

Liang-Ying Liu [a,c], Ji-Zhong Wang [a], Gao-Ling Wei [a,c], Yu-Feng Guan [b], Eddy Y. Zeng [a,*]

[a] State Key Laboratory of Organic Geochemistry, Guangzhou Institute of Geochemistry, Chinese Academy of Sciences, Guangzhou 510640, China
[b] School of Chemistry and Environment, South China Normal University, Guangzhou 510006, China
[c] Graduate School of Chinese Academy of Sciences, Beijing 100049, China

ARTICLE INFO

ABSTRACT

Sediments collected from the continental shelf of China, embracing Yellow Sea, inner shelf of the East China Sea (ECS), and the South China Sea (SCS), were analyzed for polycyclic aromatic hydrocarbons (PAHs). The concentrations of anthropogenic PAHs (Σ_{18}PAH) were 27—224 ng/g dry weight, with an average of 82 ng/g. Sedimentary PAHs in the continental shelf off China were mainly derived from mixed residues of biomass, coal, and petroleum combustion. Fluvial transport and atmospheric deposition mainly accounted for sediment PAHs in the ECS inner shelf and Yellow Sea (and the SCS), respectively. Furthermore, statistically higher levels of Σ_{18}PAH (28—224 ng/g; mean 110 ng/g) in the Yellow Sea sediment than in the SCS sediment (28—109 ng/g; mean 58 ng/g) were probably resulted from higher PAH emissions from coke industry and domestic coal combustion in North China than in South China.

© 2012 Elsevier Ltd. All rights reserved.

1. Introduction

Coastal sediments are considered as both sinks and secondary sources of terrestrially derived materials, i.e., these materials can be partially sequestered in depositional zones and partially advected into deeper waters. As a result, sediments loaded with anthropogenically derived materials, such as polycyclic aromatic hydrocarbons (PAHs), which are mainly resulted from incomplete fossil fuel and biomass burning and petroleum leakage, may be reflective of the magnitude of anthropogenic activities. Previous studies showed that PAHs can be transported to the marine environment via two main pathways, i.e., riverine runoff (Wang et al., 2007) and long-range atmospheric transport (Tsapakis et al., 2003). The relative importance of these two pathways depends largely on the distance from the input sources and on the characteristics of emitted particles. Mainly due to sedimentation, contributions from lateral transport may decrease with increasing distance (Chen et al., 2006). On the other hand, atmospheric deposition after long-range transport may become significant at distant areas (Gogou et al., 2000).

The rapid economic growth in China has magnified a variety of environmental stresses, among which mass emission of Σ_{16}PAH (16 priority pollutants identified by the United States Environmental Protection Agency (USEPA); List S1 of the Supplementary Material; "S" refers to target lists, figures and tables in the Supplementary Material thereafter) continues to rise at an alarming pace, reaching 116,000 tons in 2003 (Zhang et al., 2007). Given this gigantic amount of PAHs emitted annually in China, the outflow of even a small fraction would cause a considerable impact on the coastal marine environment. For example, our previous study estimated that China's annual riverine output of PAHs through its major rivers (e.g. Yellow River, Yangtze River, and Pearl River) amounted to 367 tons (Wang et al., 2007). Atmospheric outflow of PAHs from China was estimated to be 8092 tons/yr (Lang et al., 2008). It is well known that PAHs are carcinogenic, mutagenic and toxic to organisms and humans and widely distributed in various environmental media, which is apparently the main cause why PAHs have been comprehensively investigated (Birkholz et al., 1988; Lake et al., 1979; Larsen and Baker, 2003; Yamasaki et al., 1982). In addition, PAHs can also serve as geochemical markers for assessing anthropogenic influences within a specific environmental medium because they are closely related to anthropogenic combustion processes (Mai et al., 2003).

China's coastal zone is constituted of, from north to south, Bohai Sea, Yellow Sea, the East China Sea (ECS) and the South China Sea (SCS) (Fig. 1). A previous study (Lang et al., 2008) suggested an eastward long-range transport pathway of PAHs emitted in China,
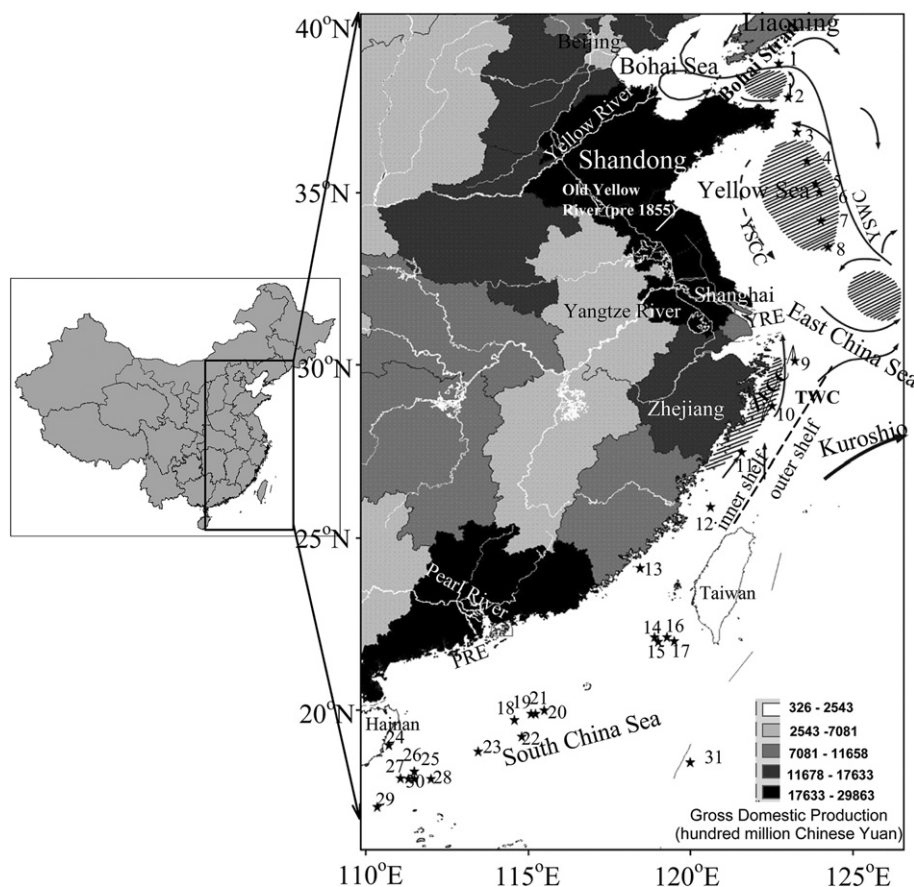
Fig. 1. Sampling sites along the continental shelf of China, covering, form north to south, Yellow Sea, inner shelf of the East China Sea and the South China Sea. The schematic diagram of mud area (stripe region) and ocean current was adopted from previous studies (Hu, 1984; Liu et al., 2007a). YSCC, YSWC, TWC, ZFCC designate the abbreviations of Yellow Sea Coastal Current, Yellow Sea Warm Current, Taiwan Warm Current, and Zhejiang-Fujian Coastal Current, respectively. YPE and PRE refer to Yangtze River Estuary and Pearl River Estuary, respectively. The filled color refers to the Gross Domestic Production (hundred million Chinese Yuan). The white curve refers to major river systems of China.

suggesting that PAHs accumulated in continental shelf sediments off China are mainly correlated with the outflows from mainland China with similar latitudes. Therefore, the regional differences in the evolution of economic development and life styles, as well as environmental factors such as ambient temperature and precipitation, provide the opportunity to assess the influences of terrestrially anthropogenic activities on the marine environment over a large spatial scale.

The objectives of the present study were to derive the concentrations and potential sources of sedimentary PAHs in the continental shelf of China, to diagnose the input mechanisms for PAHs in the study region, and to examine whether there is any correlation between the intensity of regional anthropogenic activities and the spatial distribution of PAHs along the entire continental shelf of China. It should be emphasized that the present study was the first of its kind to investigate marine sediment PAHs in such a large scale in China.

2. Materials and methods

2.1. Sample collection

Sample collection was conducted through two long-range field surveys, the South China Sea Open Cruise by R/V SHIYAN III in August 13–28, 2007 and the Open Research Cruise Offshore China by R/V KEXUE I in September 13–28, 2007. Surface sediment of ~5 cm was sampled with a stainless steel grab; samples were packed into pre-baked aluminum foils and wrapped in polyethylene bags, and preserved with ice. Once transported to the laboratory, samples were stored at −20 °C until analysis.

Geographically from north to south, three major geographical regions, Yellow Sea (sites 1–8), the ECS inner shelf (sites 9–13) and the SCS (sites 14–31) were

defined, which were sub-categorized into six groups (Table S1). Correspondingly, Shandong and further north, Shanghai and Zhejiang, Guangdong represent North, East, and South China (Fig. 1), respectively, based on the geographical classification of Chinese provinces and cities.

2.2. Sample extraction

Detailed procedures previously used (Wang et al., 2007) were followed with slight modifications. Freeze-dried samples were homogenized and assorted with an 80-mesh (mesh size: 0.18 mm) stainless steel sieve. A weighed aliquot (~25 g) of each sample was wrapped with a piece of pre-cleaned filter paper. After surrogate standards (naphthalene-d_8, acenaphthene-d_{10}, phenanthrene-d_{10}, chrysene-d_{12}, and perylene-d_{12}) and activated copper stripes for removal of elemental sulfur were added, samples were Soxhlet-extracted with 200 mL of a mixture of hexane:acetone (1:1 in volume) for 48 h. Subsequently, the extract was concentrated with a Zymark TurboVap 500 (Hopkinton, MA, USA) to approximately 2 mL, solvent-exchanged to hexane (by adding ~10 mL hexane to the extract and shaking), and then further reduced to about 1 mL. This extract was fractionated on a glass column (10 mm i.d.) packed with 6-cm alumina (lower layer) and 12-cm silica (upper layer). The fraction containing PAHs was eluted with 80 mL of hexane:dichloromethane (7:3 in volume), concentrated, solvent-exchanged to hexane, further concentrated to 0.5 mL. Internal standards (2-fluoro-1,1-biphenyl, p-terbenyl-d_{14}, and dibenzo[a,h]anthracene-d_{14} at 1 μg/mL) were added before instrumental analysis.

2.3. Instrumental analysis

Sample analysis was performed with a Shimadzu Model 2010 gas chromatograph-mass spectrometer equipped with an AOC-20i auto injector (Shimadzu, Japan) and interfaced with a 60 m × 0.25 mm-i.d. (0.25-μm film thickness) DB-5 column. Column temperature was initiated at 60 °C, ramped to 200 °C at a rate of 10 °C/min, to 214 °C at a rate of 2 °C/min, to 250 °C/min at 5 °C/min, and to 290 °C at 20 °C/min (held for 30 min). Extract injection was conducted in the splitless/split mode with a splitless time of 1 min. Injector temperature was programmed from

200 °C to 280 °C at a rate of 200 °C/min and held for 40 min. The ion source temperature was maintained at 250 °C. Mass fragments were generated in the positive electron impact mode, and scanned in the full scan mode for peak confirmation. Quantification was conducted with characteristic ions (Table S2). High purity helium was used as the carrier gas with a flow rate of 1.3 mL/min.

2.4. Measurement of total organic carbon

An aliquot (~5 g) of each sample was treated with 10% HCl to remove elemental carbon, washed with distilled water several times, and dried at 60 °C in an oven to obtain a constant weight. An elemental analyzer (Vario EL III Elementar, Germany) was used to determine total organic carbon (TOC) contents (Chen et al., 2006). Triplicate standards (acetanilide) were analyzed with each group of 20 field samples. Field samples were processed only if the relative deviations of C values from its actual value (71.09%) were less than 5% for all three standards.

2.5. Quality assurance and quality control

Three procedural blanks, two spiked blanks, and two matrix spiked samples were processed with a total of 31 field samples. Daily calibration was done by analyzing a standard solution comprised of individual PAH calibration standard compounds. The deviation of the measured concentrations from the initial calibration values must be less than 20%. The recoveries of the surrogate standards, naphthalene-d_8, acenaphthene-d_{10}, phenanthrene-d_{10}, chrysene-d_{12} and perylene-d_{12}, in the sediment samples and QA/QC samples were $50 \pm 16\%$, $62 \pm 15\%$, $77 \pm 18\%$, $90 \pm 28\%$ and $102 \pm 33\%$, respectively. The average recoveries of spiked standards (16 U.S. EPA PAHs except naphthalene) in spiked blanks and matrix spiked samples were $60 \pm 18\%$ and $57 \pm 18\%$, respectively. If the concentrations of a target analyte in the procedural blanks were greater than the lowest calibration concentration for that analyte, the mean concentration plus three standard deviations in the blanks divided by the average sample mass (20 g) was used as its reporting limit (RL). Otherwise, the lowest calibration level (20 ppb) divided by the average sample mass was defined as RL (Table S2). Measured concentrations in field samples were procedural blank corrected but not surrogate recovery corrected.

2.6. Data analysis

In the present study, a total of 28 targets PAH congeners (with full names and acronyms in Table S2) were determined, including 16 USEPA identified priority pollutants (List S1). Abnormally high levels of naphthalene and its four alkylated homologs (Table S2) were detected in several procedural blanks, while 9,10-diphenylanthracene was not detected in every sample. Therefore only the concentrations (ng/g dry wt) of the remaining 22 targets PAH compounds (List S2) were reported (Table S3). Zero was used for any measured concentration below the RL in concentration calculation, but half of the RL was used for diagnostic ratio calculation and compositional analysis. The diagnostic ratios used include BaA/(BaA + Chr), Fl/(Fl + Py), IcdP/(IcdP + BghiP), BaA/Chr, BaP/BeP and MP/P (sum of 2-mPhe, 1-mPhe, and 2,6-dimPhe to Phe). A nonparametric Mann–Whitney U test with statistical significance defined at $p < 0.05$ was used to compare the difference between two independent samples. The square of Pearson correlation coefficient (r^2) was used to display the correlation between two parameters, and $p < 0.05$ demonstrates significant relationship. All statistical analysis was performed with SPSS 13.0 (Chicago, IL, USA).

3. Results and discussion

3.1. Source assessment

Generally, PAHs in the sediment samples under investigation were mainly from the combustion of biomass, coal, and petroleum (Fig. 2), a strong indication of anthropogenic impacts (Yunker et al., 2002). In addition, there was spatial variability in these diagnostic ratios. Fl/(Fl + Py) and BaA/(BaA + Chr) shared similar distribution patterns, i.e., relatively higher in Yellow Sea than in the SCS (Fig. 2). However, such a pattern was not coherent with that of IcdP/(IcdP + BghiP), suggesting that different PAH compounds underwent different degradation pathways from source to receptor (Zhang et al., 2005). This may be why the PAH diagnostic ratios in coastal marine sediments off China deviated from those of typical combustion sources (Fig. 2). The above-mentioned spatial differences of Fl/(Fl + Py) and BaA/(BaA + Chr) possibly suggested that sediment PAHs in Yellow Sea and the SCS were derived from different sources and/or experienced different environmental
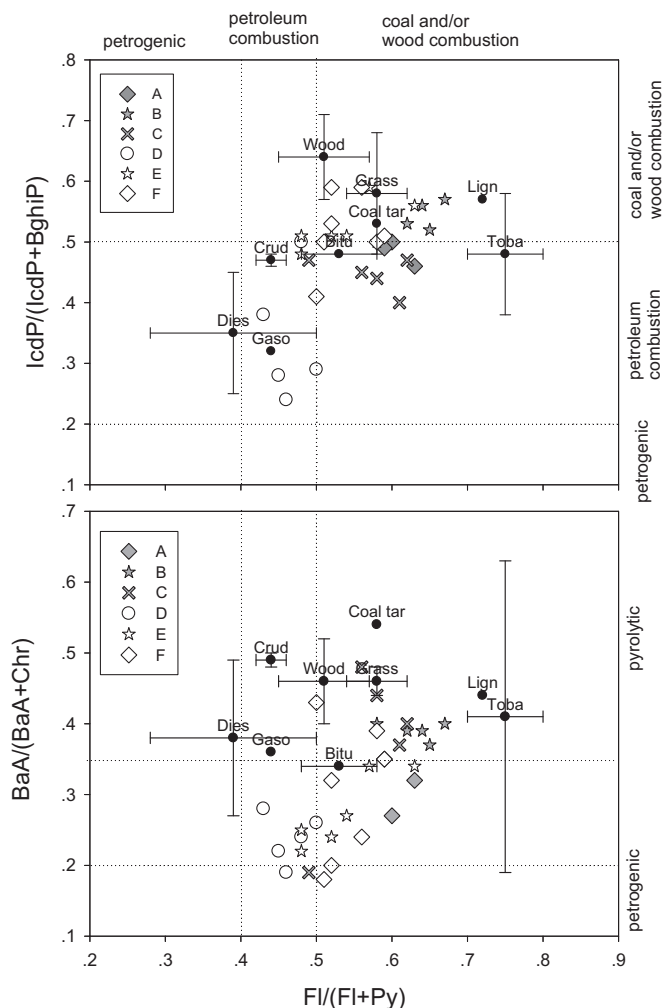
Fig. 2. Values of PAH diagnostic indices in coastal marine sediments off China and comparison with those from typical combustion sources, including grasses combustion (Grass) (Jenkins et al., 1996), wood combustion (wood) (Yunker et al., 2002), lignite and brown coal combustion (Lign) (Oros and Simoneit, 2000), bituminous coal combustion (Bitu) (Oros and Simoneit, 2000), coal tar combustion (coal tar) (Wise et al., 1988), crude oil combustion (Crud) (Benner et al., 1990), tobacco combustion (Toba) (Zhang et al., 2009), gasoline exhaust (Gaso) (Rogge et al., 1993), and diesel exhaust (Dies) (Yunker et al., 2002). The categories A (sites 1–3), B (sites 4–8), C (9–13), D (sites 14–17, 31), E (sites 18–23), and F (sites 24–30) were grouped on a basis of geographical locations (Table S1).

changes pre- and/or post deposition, which would be further discussed in the following sections.

Methylated PAH compounds can originate from low temperature combustion processes (Lake et al., 1979; Mai et al., 2003) and petrogenic residues (Mai et al., 2003; Yunker et al., 1996). Value of MP/P was less than 1 and 2–6 for pyrolytic and petrogenic PAHs, respectively (Mai et al., 2003; Zakaria et al., 2002). Higher abundance of dimethyl-phenanthrene (C2–Phe) than monomethyl-phenanthrene (C1–Phe) is indicative of fossil sources (Bouloubassi and Saliot, 1991). The MP/P and C2–/C1–Phe values in the present study were 0.41–1.25 and 0.08–0.33, respectively, which can not lead to a firm conclusion about the possible combustion sources of methylated phenanthrenes. Therefore, methylated phenanthrenes (2-mPhe, 1-mPhe, and 2,6-dimPhe) will not be included in further assessments of anthropogenic PAHs.

Perylene was detected in nearly all samples except for site 22, with concentration ranges of 2–980 ng/g (average: 65 ng/g), accounting for 3.5–96.6% (average: 26.5%) of Σ_{22}PAH (List S2). The

markedly high level of perylene at site 14 (980 ng/g) may have been resulted from oil (Yang, 2000). It was demonstrated that perylene can be formed from combustion of fossil fuels (Suzuki et al., 2010). The excellent correlations ($r^2 = 0.83–0.92$, $p = 0.01–0.03$; Table S4) between the concentrations of sedimentary peylene and anthropogenic PAHs in the ECS inner shelf suggested possible anthropogenic sources. However, previous studies excluded anthropogenic activities as the possible sources because the historical trend of perylene recorded in sediment cores differed from those of anthropogenic PAHs (Lima et al., 2003; Silliman et al., 1998). Different historical records of perylene and anthropogenic PAHs were also observed in the ECS inner shelf (Fig. S1), excluding anthropogenic activity as the possible sources of perylene. Generally, perylene is considered as either a biosynthesis product independent of precursors (Wilcke et al., 2002) or a diagenesis product from terrestrial and/or aquatic precursors (Aizenshtat, 1973; Venkatesan, 1988; Wakeham et al., 1979). Lack of significant correlations between the concentrations of perylene and anthropogenic PAHs in Yellow Sea ($r^2 = 0.02–0.21$, $p > 0.28$; Table S4) and the SCS ($r^2 = 0.04–0.14$, $p > 0.12$; Table S4) sediments suggested that perylene in these two regions was also non-anthropogenic. On the other hand, the fairly significant correlations between the concentrations of sedimentary perylene and terrestrial hydrocarbons (the sum of n-C_{27}, n-C_{29} and n-C_{31} (n-C_i, normal alkane with carbon number of i; data not shown)) in Yellow Sea ($r^2 = 0.74$, $p < 0.01$) and the SCS ($r^2 = 0.74$, $p < 0.01$) indicated that sedimentary perylene in these two regions mainly originated from diagenesis of terrestrial precursors, perylene quinones derived from fungi, insects, and black pigments in plants etc., (Aizenshtat, 1973; Bakhtiari et al., 2009; Ishiwatari et al., 1980; Silliman et al., 1998).

Based on the above assessments, methylated phenanthrenes (2-mPhe, 1-mPhe, and 2,6-dimPhe) and perylene were also excluded from the sum of individual PAHs for further discussions. The sum of the remaining 18 PAH compound (Σ_{18}PAH; List S3) was defined as anthropogenic PAHs and will be used to assess anthropogenic influences in the following sections.

3.2. Compositional patterns of anthropogenic PAHs

Fig. 3 depicted the compositional profiles of sediment Σ_{18}PAH in Yellow Sea (sites 1–8; $n = 8$), the ECS inner shelf (sites 9–13; $n = 5$), and the SCS (sites 14–31; $n = 18$). The compositional profile of sediment Σ_{18}PAH in Yellow Sea (Fig. 3a) was statistically ($r^2 = 0.34$ and $p = 0.01$) different from that in the SCS (Fig. 3c), a result of different source profiles and/or different transport mechanisms, as well as some unknown factors. Specifically, sediment samples from Yellow Sea had relatively higher concentrations (14–160 ng/g with a mean of 70 ng/g) and proportions (50–72%, mean 60% of Σ_{18}PAH) of high-molecular weight (5 + 6-ring) PAHs, while sediments from the SCS were characterized with relatively higher levels (20–190 ng/g with a mean of 53 ng/g) and proportions (42–96%, mean 67% of Σ_{18}PAH) of low to moderate molecular weight (2–4-ring) PAHs. On one hand, the compositional profiles of atmospheric PAHs in North China (Liu et al., 2007b) were different from those in Guangzhou, South China (Yang et al., 2010) (Fig. S2). On the other hand, the average temperature in North China is generally lower than that in South China (Table S5). It can be deduced that a relatively larger proportion of PAHs would be affiliated with atmospheric particulates in North China or with the gaseous phase in South China. Therefore, the different compositional profiles (Fig. 3) were likely to be caused by the region-specific source profiles and/or regional difference of gas-particle partitioning which was a function of ambient temperature (Feng et al., 2006; Liu et al., 2007b). Other unknown factors, such as benthic biota,

possibly accounted for the spatial differences of PAHs (Rust et al., 2004). Unfortunately, we can not estimate such influence due to the lack of information on the community composition and distribution, as well as on the mechanism governing the accumulation of PAHs in benthic organisms in the sampling area.

3.3. Spatial distribution of anthropogenic PAHs

Concentration ranges of anthropogenic PAHs (Σ_{18}PAH) in sediments from the continental shelf off China were 27–224 ng/g, with a median value of 57 ng/g. A preliminary comparison of sedimentary PAH concentrations with published data conducted in other coastal regions worldwide (Table S6) indicated that sedimentary PAH concentrations in the continental shelf of China were at the low to moderate levels of the global range. Overall, the sediments of the upper ECS inner shelf (96–210 ng/g, with a median of 180 ng/g; sites 10–12) and central Yellow Sea (53–224 ng/g, with a median of 129 ng/g; sites 4–8) contained higher levels of Σ_{18}PAH than those of northern Yellow Sea (27–110 ng/g, with a median of 51 ng/g; sites 1–3), the lower ECS inner shelf (54 ng/g; site 13) and the SCS (28–109 ng/g, with a median of 57 ng/g; sites 14–31) (Fig. 4). On a larger scale, the Σ_{18}PAH concentrations in the Yellow Sea sediments were statistically ($p < 0.05$) higher than those in the SCS (except for site 17) (Fig. 4).

Specifically, much lower Σ_{18}PAH concentrations (50 and 54 ng/g, respectively) at sites 9 and 13 located at the eastward and southward offshore areas of the Yangtze River Estuary than those at upper region of the ECS inner shelf (sites 10–12; Fig. 4) suggested that the former received minor anthropogenic inputs. The comparable and low levels of Σ_{18}PAH at sites 9 and 13 may represent background levels of atmospheric deposition since the eastwardly hydrodynamic transport of terrestrial inputs from the Yangtze River was obstructed by the southward coastal current (Fig. 1). Similar background level was observed in sediments (50 ng/g) along the entire coast of Thailand (Boonyatumanond et al., 2006), and in aquatic sediments ($\sim$50 to $\sim$100 ng/g) in eight tropical Asian countries (Saha et al., 2009). The southward alongshore decreasing trend of Σ_{18}PAH (sites 10–13; Fig. 4) was in alignment with the prevailing coastal current that transports materials discharged from the Yangtze River along the coast (Guan et al., 1998; Liu et al., 2007a), suggesting that hydrodynamic transport may have been the dominant input mechanism responsible for the spatial distribution of anthropogenic PAHs along the ECS inner shelf.

3.4. Assessment of transport mechanisms

The old Yellow River Delta is expected to contain insignificant anthropogenic pollutants because Yellow River changed its course to Bohai Sea in 1855 before the era of industrialization in China (Guo et al., 2001; Milliman et al., 1985). Sites 4–8 are located in the Yellow Sea mud areas (Fig. 1), which received discharges from the old Yellow River Delta (Guo et al., 2001; Milliman et al., 1985). The lower levels of sediment Σ_{18}PAH in northern Yellow Sea (sites 1–3) than in central Yellow Sea (Fig. 4) suggested that hydrodynamic transport was not the dominant input mechanism. In addition, a previous study also suggested that atmospheric input was more important than riverine input in transporting metals to the Yellow Sea (Zhang et al., 1992). Moreover, the compositional profile of sediment PAHs in Yellow Sea was dominated by high-molecular weight (5 + 6-ring) PAHs (50–72% with a mean of 60%; Fig. 3a), which are largely transported with particles. Thus, PAHs in the Yellow Sea sediments were contributed largely from atmospheric input, especially via particle deposition. This was in accordance with the lower precipitation, especially during winter seasons in North China (Table S5), which facilitated outflow of particles.
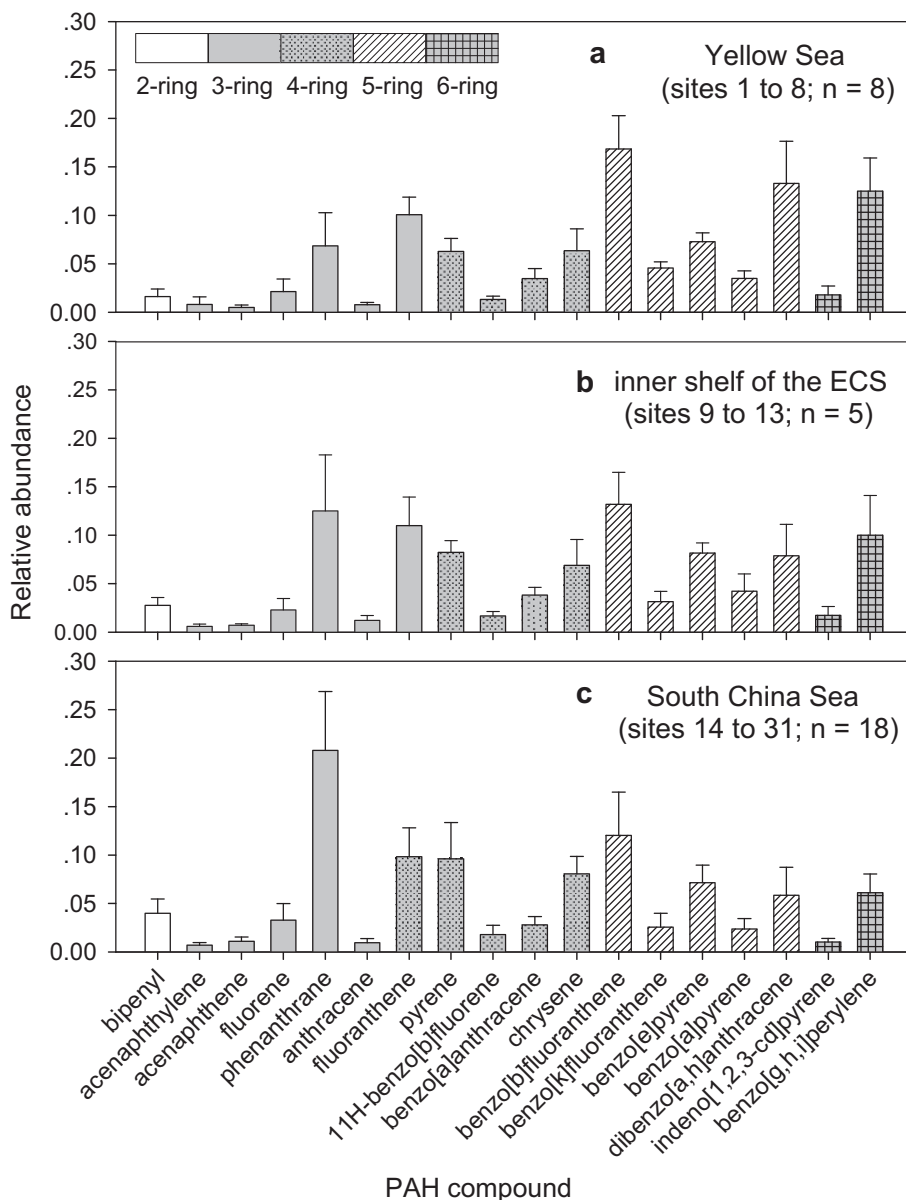
Fig. 3. Relative abundance of each PAH compound normalized to Σ_{18}PAH in continental shelf sediments of China from (a) Yellow Sea (sites 1 to 8; $n = 8$), (b) inner shelf of the East China Sea (ECS) (sites 9 to 13; $n = 5$) and (c) the South China Sea (sites 14 to 31; $n = 18$) (Fig. 1). The bars and errors represent means and standard deviations, respectively.

The anthropogenic influence by fluvial transport from the Pearl River Delta on the northern SCS was estimated to reach as far as 124–276 km from the Pearl River Estuary (Chen et al., 2006). Samples in the SCS were collected with a distance of at least 280 km from the coastline of China; therefore contributions from riverine runoff were expected to be minor. The concentrations of Σ_{18}PAH in the SCS (28–109 ng/g with an average of 57 ng/g; Table S3) were comparable to or slightly higher than the background level (50 ng/g at site 9) from atmospheric inputs, suggesting minor impact from riverine input. Therefore, PAHs accumulated in the SCS sediments were also mainly derived from long-range atmospheric transport. Moreover, the highest relative abundance of phenanthrene in most samples from the SCS (Fig. 3) was similar to that from the central Atlantic sediment (Ohkouchi et al., 1999) where pyrolytic PAHs mainly originated from atmospheric deposition. In summary, PAHs accumulated in the Yellow Sea and SCS sediments were mainly derived from long-range atmospheric transport.

3.5. Reference to terrestrial emission intensity

Atmospheric deposition flux other than factors such as water content and sedimentation rate was believed to be the primary controlling factor for the two orders of magnitude higher PAH levels in sediments in higher latitude (27°N–48°N) than in lower latitude (15°S–24°N) of the central Pacific (Ohkouchi et al., 1999). The generally higher levels of anthropogenic PAHs in Yellow Sea than in the SCS (Fig. 4) was possibly resulted from regional input source intensity, as well as a combination of environmental factors, such as sedimentation rate, sediment organic carbon content (Arzayus et al., 2001; Yang, 2000), extent of photo-degradation during atmospheric transport, and pre-depositional decomposition occurring in the water column. In fact, atmospheric PAH concentrations (Table S7) were higher in North China than in South China, which is probably a reflection of the variable life styles and economic development paths, which will be discussed in detail below.
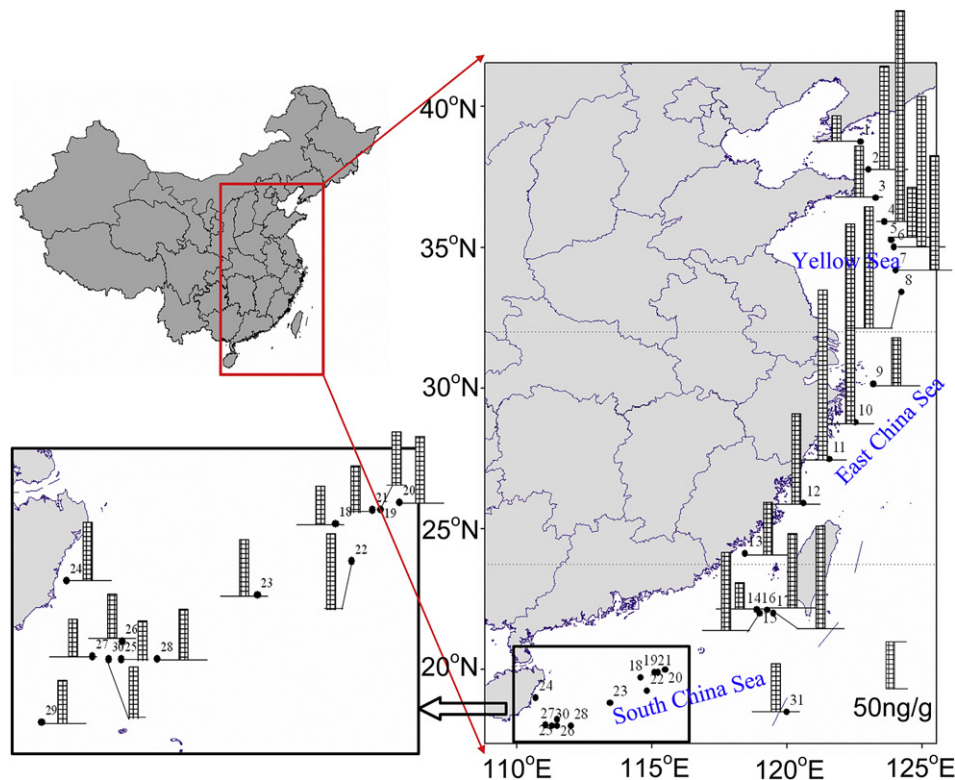
Fig. 4. Spatial distribution of anthropogenic PAHs (Σ_{18}PAH; List S3) in continental shelf sediments of China. Two horizontal dotted lines separated samples from Yellow Sea, inner shelf of the East China Sea and the South China Sea.

Although the energy structures vary among provinces, coal is the dominant energy source (>50%; Fig. 5) in China. Obviously, North China has consumed larger amounts of coal and coke while fewer amounts of gasoline, kerosene, diesel and liquefied petroleum gas (Fig. 5) than South China. The cold winter weather in North China requires an additional amount of coal for space heating (Fig. 5), thus resulting in relatively higher Σ_{16}PAH emissions from both industrial and domestic coal combustion in North China than in South China (Fig. 6) (Xu et al., 2006). It is noteworthy that the emissions from industrial coal combustion constitute only a minor fraction of the total emissions (Fig. 6). Instead, the low efficiency with domestic coal combustion (Liu et al., 2007c) and the greater consumption of domestic coal in North China compared to South China (e.g. 6.2 and 0.69 million tons in Shandong (Statisticcal Bureau of Shandong Province, 2009) and Guangdong (Statistical Bureau of Guangdong Province, 2010), respectively) were probably responsible for the spatial distribution of anthropogenic PAH in continental shelf sediments off China (Fig. 4), which may also have been caused by the larger emissions of Σ_{16}PAH from coke industry (Fig. 6) in North China. Another important source emission of Σ_{16}PAH was biomass combustion (Fig. 6), which was consistent with the results deduced under the section of 'Source Assessment'. However, the comparable emissions of Σ_{16}PAH between North and South China (Fig. 6) excluded emission from biomass combustion as a reason for the spatial distribution of anthropogenic PAHs (Fig. 4). In summary, the greater emissions from domestic coal combustion and coke industry were probably responsible for the higher anthropogenic PAHs levels in Yellow Sea than in the SSC sediments (Fig. 4). Consequently, sediment pollution in Yellow Sea may be alleviated by increased combustion efficiency with domestic coal combustion and replacement of coal with liquefied petroleum gas as the residential energy in North China.
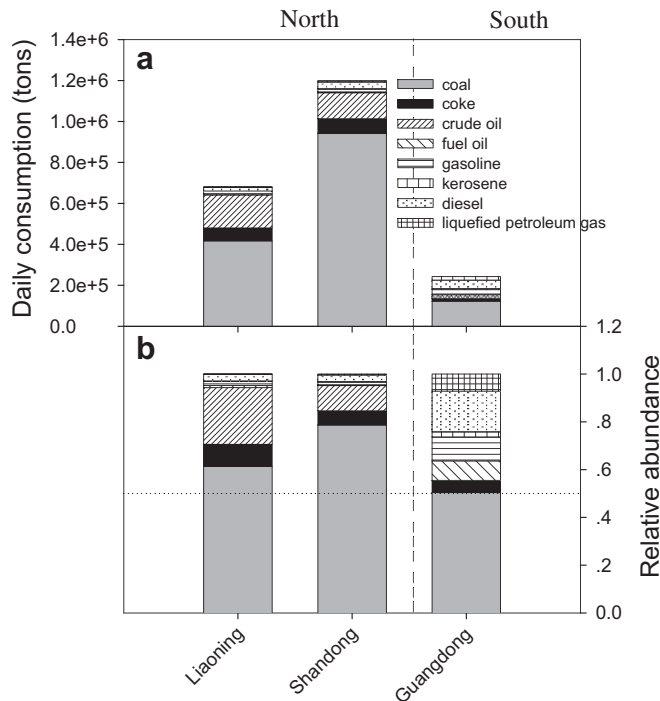

Fig. 5. (a) Average daily consumption of major energy types and (b) relative contribution of each energy type to the total energy consumption in coastal provinces of China, including Liaoning (Statisticcal Bureau of Liaoning Province, 2009), Shandong (Statisticcal Bureau of Shandong Province, 2009), and Guangdong (Statistical Bureau of Guangdong Province, 2010). The vertical-dashed line separated the North and South China, while the horizontal dotted line suggested that coal accounts for at least half of the total energy consumption.
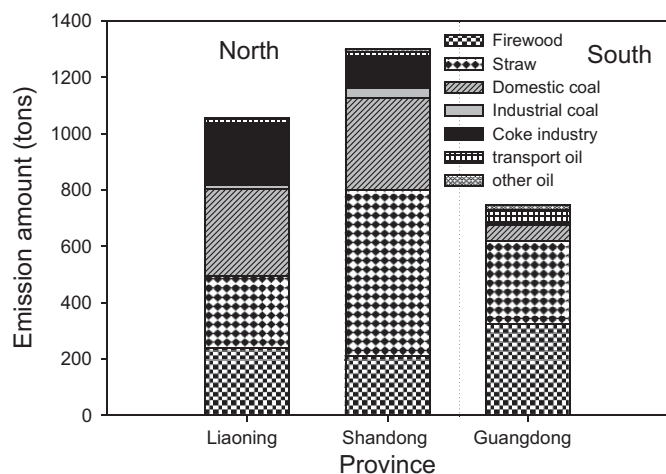
Fig. 6. The emission amounts (tons) of Σ_{16}PAH (List S1) from major combustion sources (firewood, straw, domestic coal, industrial coal, coke industry, aluminum manufacture, transport oil and other oil) in coastal provinces (Liaoning and Shandong in North; Guangdong in South) of China. PAH emission data are compiled and re-analyzed (multiply energy consumption and its corresponding combustion emission factor) from a previous study (Xu et al., 2006).

The PAH concentrations in sediment cores from Yellow Sea were generally greater than those from the SCS within the sediment column although the sedimentation rates between Yellow Sea and the SCS were different (0.3 and 0.2 cm/yr, respectively, based on ^{210}Pb activity) (unpublished data). Therefore, different sedimentation rates at different sampling locations are expected to have insignificant impacts on the spatial distribution patterns of PAH compositions and concentration levels. Poor correlation between Σ_{18}PAH concentrations and TOC ($r^2 = 0.01$; $p = 0.66$) ruled out sediment TOC as the controlling factor in the study region. This potentially implicated the role of black carbon (Oen et al., 2006; Sánchez-García et al., 2010) as an important factor governing environmental distribution of PAHs. The extent of photo-degradation can be diagnosed using the ratios of BaA/Chr and BaP/BeP, as BaA and BaP can be more easily photo-degraded than Chr and BeP (Ding et al., 2007). The lower values of BaA/Chr and BaP/BeP (Fig. S3) in the SCS sediments than in the Yellow Sea sediments indicated that PAHs accumulated in the SCS sediments had been subject to greater photo-degradation during long-range atmospheric transport. However, the poor correlation ($r^2 = 0.3$ or 0.006) between BaA/Chr or BaP/BeP and Σ_{18}PAH (List S3) suggested that decomposition during atmospheric transport was not the main mechanism leading to the spatial distribution (Fig. 4). Polycyclic aromatic hydrocarbons are associated with particulate matter such as fecal pellets of zooplankton and downward transported to sediments after entering into the water column (Prahl and Carpenter, 1979). During the sinking process, PAHs, especially low-molecular weight (LMW) PAHs (e.g. phenanthrene), are subject to micro-degradation (Juhasz and Naidu, 2000; Ohkouchi et al., 1999), which is partly influenced by the time length of exposure to microorganisms. The sampling sites in the SCS are located at deeper water depths (65–2456 m; Table S1) than those in Yellow Sea (53.8–80.4 m; Table S1), but the levels of phenanthrene in the SCS sediment (5.3–22.6 ng/g with an average of 12.2 ng/g) were higher than those in the Yellow Sea sediment (1.3–13.7 ng/g with an average of 6.9 ng/g), suggesting lower degree of decomposition in the SCS than in Yellow Sea. This discrepancy somewhat implicated that decomposition during the sinking process was also not the main cause leading to the spatial distribution of anthropogenic PAHs (Fig. 4).

4. Conclusions

Continental shelf sediments of China contained low to moderate levels of anthropogenic PAHs compared to other shelf regions worldwide. Spatial differences of PAH compositions and concentrations were observed between Yellow Sea and the SCS. The different source profiles of PAHs, as well as the difference in gas-particle partitioning caused by regionally different ambient temperatures between North China and South China, mainly accounted for the spatial divergences of sedimentary PAH compositions, but other unknown factors could not be completely excluded. Greater PAH emissions from domestic coal combustion and coke industry in North China than in South China may have been responsible for the general higher sedimentary PAH levels in Yellow Sea sediments than in the SCS.

Appendix A. Supplementary material

Supplementary data associated with this article can be found, in the online version, at doi:10.1016/j.envpol.2012.03.038.

References

Aizenshtat, Z., 1973. Perylene and its geochemical significance. Geochimica et Cosmochimica Acta 37, 559–567.

Arzayus, K.M., Dickhut, R.M., Canuel, E.A., 2001. Fate of atmospherically deposited polycyclic aromatic hydrocarbons (PAHs) in Chesapeake Bay. Environmental Science and Technology 35, 2178–2183.

Bakhtiari, A.R., Zakaria, M.P., Yaziz, M.I., Lajis, M.N.H., Bi, X.-H., Rahim, M.C.A., 2009. Vertical distribution and source identification of polycyclic aromatic hydrocarbons in anoxic sediment cores of Chini Lake, Malaysia: perylene as indicator of land plant-derived hydrocarbons. Applied Geochemistry 24, 1777–1787.

Benner, B.A., Bryner, N.P., Wise, S.A., Mulholland, G.W., Lao, R.C., Fingas, M.F., 1990. Polycyclic aromatic hydrocarbon emissions from the combustion of crude oil on water. Environmental Science and Technology 24, 1418–1427.

Birkholz, D.A., Coutts, R.T., Hrudey, S.E., 1988. Determination of polycyclic aromatic compounds in fish tissue. Journal of Chromatography A 449, 251–260.

Boonyatumanond, R., Wattayakorn, G., Togo, A., Takada, H., 2006. Distribution and origins of polycyclic aromatic hydrocarbons (PAHs) in riverine, estuarine, and marine sediments in Thailand. Marine Pollution Bulletin 52, 942–956.

Bouloubassi, I., Saliot, A., 1991. Sources and transport of hydrocarbons in the Rhone delta sediments (Northwestern Mediterranean). Fresenius' Journal of Analytical Chemistry 339, 765–771.

Chen, S.-J., Luo, X.-J., Mai, B.-X., Sheng, G.-Y., Fu, J.-M., Zeng, E.Y., 2006. Distribution and mass inventories of polycyclic aromatic hydrocarbons and organochlorine pesticides in sediments of the Pearl River Estuary and the northern South China Sea. Environmental Science and Technology 40, 709–714.

Ding, X., Wang, X.-M., Xie, Z.-Q., Xiang, C.-H., Mai, B.-X., Sun, L.-G., Zheng, M., Sheng, G.-Y., Fu, J.-M., Pöschl, U., 2007. Atmospheric polycyclic aromatic hydrocarbons observed over the North Pacific Ocean and the Arctic area: spatial distribution and source identification. Atmospheric Environment 41, 2061–2072.

Feng, J.-L., Hu, M., Chan, C.K., Lau, P.S., Fang, M., He, L.-Y., Tang, X.-Y., 2006. A comparative study of the organic matter in PM2.5 from three Chinese megacities in three different climatic zones. Atmospheric Environment 40, 3983–3994.

Gogou, A., Bouloubassi, I., Stephanou, E.G., 2000. Marine organic geochemistry of the Eastern Mediterranean: 1. Aliphatic and polyaromatic hydrocarbons in Cretan Sea surficial sediments. Marine Chemistry 68, 265–282.

Guan, W.B., Wolanski, E., Dong, L.X., 1998. Cohesive sediment transport in the Jiaojiang River estuary, China. Estuarine, Coastal and Shelf Science 46, 861–871.

Guo, Z.-G., Yang, Z.-S., Chen, Z.-L., Mao, D., 2001. Source of sedimentary organic matter in the mud areas of the East China Sea shelf. Geochimia 30, 416–424 (in Chinese).

Hu, D.-X., 1984. Unpwelling and sedimentation dynamics: I. The role of upwelling in sedimentation in the Huanghai Sea and East China Sea-A description of general features. Journal of Oceanology and Limnology 2, 13–19.

Ishiwatari, R., Ogura, K., Horie, S., 1980. Organic geochemistry of a lacustrine sediment (Lake Haruna, Japan). Chemical Geology 29, 261–280.

Jenkins, B.M., Jones, A.D., Turn, S.Q., Williams, R.B., 1996. Emission factors for polycyclic aromatic hydrocarbons from biomass burning. Environmental Science and Technology 30, 2462–2469.

Juhasz, A.L., Naidu, R., 2000. Bioremediation of high molecular weight polycyclic aromatic hydrocarbons: a review of the microbial degradation of benzo[a]pyrene. International Biodeterioration & Biodegradation 45, 57–88.

Lake, J.L., Norwood, C., Dimock, C., Robert, B., 1979. Origins of polycyclic aromatic hydrocarbons in estuarine sediments. Geochimica et Cosmochimica Acta 43, 1847–1854.

Lang, C., Tao, S., Liu, W.-X., Zhang, Y.-X., Simonich, S., 2008. Atmospheric transport and outflow of polycyclic aromatic hydrocarbons from China. Environmental Science and Technology 42, 5196–5201.

Larsen, R.K., Baker, J.E., 2003. Source apportionment of polycyclic aromatic hydrocarbons in the urban atmosphere: a comparison of three methods. Environmental Science and Technology 37, 1873–1881.

Lima, A.L.C., Eglinton, T.I., Reddy, C.M., 2003. High-resolution record of pyrogenic polycyclic aromatic hydrocarbon deposition during the 20th century. Environmental Science and Technology 37, 53–61.

Liu, J.-P., Xu, K.-H., Li, A.-C., Milliman, J.D., Velozzi, D.M., Xiao, S.-B., Yang, Z.-S., 2007a. Flux and fate of Yangtze River sediment delivered to the East China Sea. Geomorphology 85, 208–224.

Liu, S.-Z., Tao, S., Liu, W.-X., Liu, Y.-N., Dou, H., Zhao, J.-Y., Wang, L.-G., Wang, J.-F., Tian, Z.-F., Gao, Y., 2007b. Atmospheric polycyclic aromatic hydrocarbons in North China: a winter-time study. Environmental Science and Technology 41, 8256–8261.

Liu, X., Zhang, G., Li, J., Cheng, H.-R., Qi, S.-H., Li, X.-D., Jones, K.C., 2007c. Polycyclic aromatic hydrocarbons (PAHs) in the air of Chinese cities. Journal of Environmental Monitoring 9, 1092–1098.

Mai, B.-X., Qi, S.-H., Zeng, E.Y., Yang, Q.-S., Zhang, G., Fu, J.-M., Sheng, G.-Y., Peng, P.-A., Wang, Z.-S., 2003. Distribution of polycyclic aromatic hydrocarbons in the coastal region off Macao, China: assessment of input sources and transport pathways using compositional analysis. Environmental Science and Technology 37, 4855–4863.

Milliman, J.D., Huang-ting, S., Zuo-sheng, Y., Mead, R.H., 1985. Transport and deposition of river sediment in the Changjiang estuary and adjacent continental shelf. Continental Shelf Research 4, 37–45.

Oen, A.M.P., Cornelissen, G., Breedveld, G.D., 2006. Relation between PAH and black carbon contents in size fractions of Norwegian harbor sediments. Environmental Pollution 141, 370–380.

Ohkouchi, N., Kawamura, K., Kawahata, H., 1999. Distributions of three- to seven-ring polynuclear aromatic hydrocarbons on the deep sea floor in the central Pacific. Environmental Science and Technology 33, 3086–3090.

Oros, D.R., Simoneit, B.R.T., 2000. Identification and emission rates of molecular tracers in coal smoke particulate matter. Fuel 79, 515–536.

Prahl, F.G., Carpenter, R., 1979. The role of zooplankton fecal pellets in the sedimentation of polycyclic aromatic hydrocarbons in Dabob Bay, Washington. Geochimica et Cosmochimica Acta 43, 1959–1972.

Rogge, W.F., Hildemann, L.M., Mazurek, M.A., Cass, G.R., Simoneit, B.R.T., 1993. Sources of fine organic aerosol. 2. Noncatalyst and catalyst-equipped automobiles and heavy-duty diesel trucks. Environmental Science and Technology 27, 636–651.

Rust, A.J., Burgess, R.M., Brownawell, B.J., McElroy, A.E., 2004. Relationship between metabolism and bioaccumulation of benzo[a]pyrene in benthic invertibrates. Environmental Toxicology and Chemistry 23, 2587–2593.

Sánchez-García, L., Cato, I., Gustafsson, Ö., 2010. Evaluation of the influence of black carbon on the distribution of PAHs in sediments from along the entire Swedish continental shelf. Marine Chemistry 119, 44–51.

Saha, M., Togo, A., Mizukawa, K., Murakami, M., Takada, H., Zakaria, M.P., Chiem, N.H., Tuyen, B.C., Prudente, M., Boonyatumanond, R., Sarkar, S.K.,

Bhattacharya, B., Mishra, P., Tana, T.S., 2009. Sources of sedimentary PAHs in tropical Asian waters: differentiation between pyrogenic and petrogenic sources by alkyl homolog abundance. Marine Pollution Bulletin 58, 189–200.

Silliman, J.E., Meyers, P.A., Eadie, B.J., 1998. Perylene: an indicator of alteration processes or precursor materials? Organic Geochemistry 29, 1737–1744.

Statistical Bureau of Guangdong Province, 2010. Guangdong Statistical Yearbook 2009.

Statistical Bureau of Liaoning Province, 2009. Liaoning Statistical Yearbook 2008. China Statistics Press, Beijing.

Statisticcal Bureau of Shandong Province, 2009. Shandong Statistical Yearbook 2009. China Statistics Press, Beijing.

Suzuki, N., Yessalina, S., Kikuchi, T., 2010. Probable fungal origin of perylene in Late Cretaceous to Paleogene terrestrial sedimentary rocks of northeastern Japan as indicated from stable carbon isotopes. Organic Geochemistry 41, 234–241.

Tsapakis, M., Stephanou, E.G., Karakassis, I., 2003. Evaluation of atmospheric transport as a nonpoint source of polycyclic aromatic hydrocarbons in marine sediments of the Eastern Mediterranean. Marine Chemistry 80, 283–298.

Venkatesan, M.I., 1988. Occurrence and possible sources of perylene in marine sediments-a review. Marine Chemistry 25, 1–27.

Wakeham, S.G., Schaffner, C., Giger, W., Boon, J.J., De Leeuw, J.W., 1979. Perylene in sediments from the Namibian shelf. Geochimica et Cosmochimica Acta 43, 1141–1144.

Wang, J.-Z., Guan, Y.-F., Ni, H.-G., Luo, X.-L., Zeng, E.Y., 2007. Polycyclic aromatic hydrocarbons in riverine runoff of the Pearl River Delta (China):concentrations, fluxes, and fate. Environmental Science and Technology 41, 5614–5619.

Wilcke, W., Krauss, M., Amelung, W., 2002. Carbon isotope signature of polycyclic aromatic hydrocarbons (PAHs): evidence for different sources in tropical and temperate environments? Environmental Science and Technology 36, 3530–3535.

Wise, S.A., Benner, B.A., Byrd, G.D., Chesler, S.N., Rebbert, R.E., Schantz, M.M., 1988. Determination of polycyclic aromatic hydrocarbons in a coal tar standard reference material. Analytical Chemistry 60, 887–894.

Xu, S.-S., Liu, W.-X., Tao, S., 2006. Emission of polycyclic aromatic hydrocarbons in China. Environmental Science and Technology 40, 702–708.

Yamasaki, H., Kuwata, K., Miyamoto, H., 1982. Effects of ambient temperature on aspects of airborne polycyclic aromatic hydrocarbons. Environmental Science and Technology 16, 189–194.

Yang, G.-P., 2000. Polycyclic aromatic hydrocarbons in the sediments of the South China Sea. Environmental Pollution 108, 163–171.

Yang, Y.-Y., Guo, P.-R., Zhang, Q., Li, D.-L., Zhao, L., Mu, D.-H., 2010. Seasonal variation, sources and gas/particle partitioning of polycyclic aromatic hydrocarbons in Guangzhou, China. Science of the Total Environment 408, 2492–2500.

Yunker, M.B., Macdonald, R.W., Vingarzan, R., Mitchell, R.H., Goyette, D., Sylvestre, S., 2002. PAHs in the Fraser River basin: a critical appraisal of PAH ratios as indicators of PAH source and composition. Organic Geochemistry 33, 489–515.

Yunker, M.B., Snowdon, L.R., Macdonald, R.W., Smith, J.N., Fowler, M.G., Skibo, D.N., McLaughlin, F.A., Danyushevskaya, A.I., Petrova, V.I., Ivanov, G.I., 1996. Polycyclic aromatic hydrocarbon composition and potential sources for sediment samples from the Beaufort and Barents seas. Environmental Science and Technology 30, 1310–1320.

Zakaria, M.P., Takada, H., Tsutsumi, S., Ohno, K., Yamada, J., Kouno, E., Kumata, H., 2002. Distribution of polycyclic aromatic hydrocarbons (PAHs) in rivers and estuaries in Malaysia: a widespread input of petrogenic PAHs. Environmental Science and Technology 36, 1907–1918.

Zhang, J., Hunag, W.-W., Zhang, J., Wang, Q., 1992. Transport of particulate heavy metals towards the east China Seas: a preliminary study and comparison. Marine Chemistry 40, 161–178.

Zhang, L.-W., Bai, Z.-P., You, Y., Wu, J.-H., Feng, Y.-C., Zhu, T., 2009. Chemical and stable carbon isotopic characterization for PAHs in aerosol emitted from two indoor sources. Chemosphere 75, 453–461.

Zhang, X.-L., Tao, S., Liu, W.-X., Yang, Y., Zuo, Q., Liu, S.-Z., 2005. Source diagnostics of polycyclic aromatic hydrocarbons based on species ratios: a multimedia approach. Environmental Science and Technology 39, 9109–9114.

Zhang, Y.-X., Shao, M., Zhang, Y.-H., Zeng, L.-M., He, L.-Y., Zhu, B., Wei, Y.-J., Zhu, X.-L., 2007. Source profiles of particulate organic matters emitted from cereal straw burnings. Journal of Environmental Sciences 19, 167–175.